Biomicrofluidics ARTICLE scitation.org/journal/bmf

Simple and low-cost production of hybrid 3D-printed microfluidic devices

Cite as: Biomicrofluidics 13, 024108 (2019); doi: 10.1063/1.5092529
Submitted: 11 February 2019 · Accepted: 8 April 2019 ·
Published Online: 23 April 2019

Lynh Huyen Duong and Pin-Chuan Chen[a)]

AFFILIATIONS

Department of Mechanical Engineering, National Taiwan University of Science and Technology, Taipei 10607, Taiwan

[a)]Pcchen@mail.ntust.edu.tw. **Tel.:** 886-2-27376456. **Fax:** 886-2-27376460.

ABSTRACT

The use of three-dimensional (3D) printing for the fabrication of microfluidic chips has attracted considerable attention among researchers. This low-cost fabrication method allows for rapid prototyping and the creation of complex structures; however, these devices lack optical transparency, which greatly hinders the characterization and quantification of experiment results. To address this problem, integrating a transparent substrate with a 3D-printed chip is an effective approach. In this study, we present a solvent bonding method of poly(methyl methacrylate) (PMMA) and acrylonitrile butadiene styrene (ABS) thermoplastic materials for the creation of optically detectable 3D-printed microfluidic devices. To achieve an excellent bonding between PMMA and ABS substrates, we used spray coating as a method for the distribution of ethanol solution followed by UV exposure and post-annealing step to improve the bonding strength. We fabricated a microfluidic chip with S-microchannel to characterize the bonding protocol, and other two application-oriented microfluidic chips, including a 3D split-and-recombine-based passive micromixer, and an integrated microchip for the mixing of two streams of liquid prior to the formation of double-emulsion droplets, to evaluate the efficacy of the proposed scheme. As a result, at least eight bars of the bonding strength between PMMA/ABS substrates was achieved, and the ability of producing optically detectable 3D-printed microfluidic devices based on this bonding method was confirmed.

I. INTRODUCTION

Three-dimensional (3D) printing can be defined as "an additive process of joining materials layer upon layer to make parts from 3D model data, usually, as opposed to subtractive manufacturing and formative manufacturing methodologies" (ISO/ASTM 52900:2015). It is expected that between 2017 and 2023, the 3D printing market will grow to USD 32.78 billion, based on a CAGR (compound annual growth rate) of 25.76%.[1] This growth can largely be attributed to the ease with which products can be customized, the ability to reduce overall manufacturing costs, and government investment in 3D printing projects aimed at advancing the deployment of this technology.

The application of 3D manufacturing to the fabrication of microfluidic devices has gained considerable attention.[2–13] Compared to conventional fabrication methods (e.g., photolithography), this technology enables faster prototyping, shorter lead times for manufacturing, and lower production costs. However, optical transparency is often a problem in the 3D printing of microfluidic chips.[14,15] This can be attributed to the fact that the optical clarity (i.e., transparency) of a printed device depends on the absorption of light by the material as well as roughness of the surface and defects within the printed bulk material, both of which can cause light diffraction. Despite improvements in print resolution and polishing techniques, the stacking of layers still leads to light scattering. In short, it is practically impossible to render the interior of a microchannel transparent simply through the adoption of ostensibly transparent materials.

The incorporation of glass or transparent thermoplastic materials (e.g., PMMA) is another approach to the creation of transparent 3D-printed devices. Takenaga *et al.* assembled a stereolithography (STL)-printed microfluidic unit on a light-addressable potentiometric sensor (LAPS) for cell culturing by using photo resin as adhesive material.[16] Wardyn *et al.* used a biocompatible glue (NEB, SYLGARD® 184) or a parafilm to seal a printed polylactic acid (PLA) component to a glass cover slip for the culturing of primary neurons.[17] These two methods were simple, however, using glue to incorporate a glass substrate into the PLA component may cause the clogging of the microchannel. Salentijn *et al.* inserted a glass slide during printing process (i.e., the printer was paused) to seal PLA channels. This approach was straightforward, but leakage was observed along the edges of the PLA channel where it contacted the glass slide.[18] Bertana *et al.* used a customized STL printer to print microfluidic channels enclosed between

two PMMA layers in a sandwichlike structure. For microfluidic walls, two distinct commercial resins with different properties were used including STBlend (FunToDo) and spotHT resin (SpotAmaterial). In experiments, they achieved bonding strength between PMMA/STBlend of 2 bars.[19]

In this study, we present a solvent bonding method for rapid incorporation of the ABS component with complex 3D features into an excellent optically transparent PMMA, a thermoplastic material commonly used for microfluidics, thanks to its compatibility with solvents and chemicals and well-understood molding parameters.[20] A fused deposition modeling (FDM) printer was used to print complex structures on ABS, which is widely used in 3D printing. ABS and PMMA substrates were spray-coated a layer of ethanol solution, as solvent, then followed UV exposure and post-annealing step to form a strong bond. Scanning electron microscopy (SEM), leakage tests, and burst tests were used to validate the bonded microfluidic chips, and several investigations were conducted to characterize the bonding protocol. Based on this solvent bonding method, we can create hybrid ABS/PMMA microfluidic chips which provide a number of side benefits: (1) connectors can be embedded during 3D printing to eliminate the troublesome task of assembling tubing during the execution of experiments; and (2) channels on the PMMA side can be fabricated at micro/sub-micro/nanoscales without having to deal with current limitations pertaining to 3D printing resolution.[21–25] To demonstrate the benefits of the proposed bonding technique, two microfluidic devices were then fabricated: (a) a 3D SAR-based passive micromixer and (b) an integrated chip with a micro mixing system and double-emulsion generator.

II. MATERIALS AND METHODS

A. ABS material properties and FDM printing strategy

ABS is an important engineering thermoplastic with glass transition temperature of approximately 105 °C.[26,27] This material contains a butadiene component uniformly distributed over an acrylonitrile–styrene matrix in the following proportions: acrylonitrile (15%–30%), styrene (40%–60%), and poly butadiene rubber (5%–30%).[28,29] This combination of materials gives ABS excellent toughness, even in cold conditions, such as cryogenic applications.[30] It also provides good rigidity, good thermal stability, and high resistance to chemicals and cracking due to environmental stress. ABS is inexpensive, flexible, lightweight, and easily extruded, which makes it perfect for 3D printing. In fact, ABS has been a mainstay in this field since its inception.

Nonetheless, the use of ABS in the fabrication of microfluidic devices raises a number of concerns. Microfluidic devices are applied primarily in biology, wherein biocompatibility is a critical issue. Researchers have demonstrated that ABS can have cytotoxic effects on human neuroblastoma cells and mouse pituitary cells[31] and influence the functionality of cortical neurons. However, in a recent study (2017), Salentijn *et al.* failed to observe any negative effects of ABS on the HUVEC (human umbilical vein endothelia cells) or PCLS (precision cut liver slices) models.[18] Even poly(lactic acid) (PLA), which is well-known for its biocompatibility, has been shown to affect the central nervous system and skin cells as well as drug delivery and carcinogenicity.[32] Regardless of these findings, there is strong evidence to support the use of ABS for many biological applications. In one study, ABS was used as a bioreceptive polymer for directing the C_2C_{12} cellular phenotype *in vitro*.[33] In another study, ABS was used to print scaffolds for the regeneration of cartilage and nucleus pulposus tissue.[34]

FDM is the primary approach to printing ABS objects. This low-cost method involves the heating and extrusion of thermoplastic material through a motor-driven nozzle head that is movable in three dimensions, which then undergoes immediate hardening via spontaneous cooling. In this study, we employed an FDM-3D printer (Printech 200, Taiwan Teama Technology Co., Ltd, Taiwan) and ABS filaments with a diameter of 1.75 mm ± 0.05 mm (Voltivo, Germany) for the printing of microfluidic structures. The layer resolution of this printer is 100 μm (Z-axis), and the diameter of the nozzle is 400 μm. The temperature for extrusion nozzle was set at 250 °C. Setting the temperature of the print bed too low would increase the risk of warping due to variations in the internal temperature of printed objects, which could result in detachment from the print bed. Thus, we set the temperature of the print bed at 90–105 °C and employed a number of methods to reduce or prevent warping. (1) We covered the top of the 3D printer with a modified carton to prevent the convection through air in order to maintain a more uniform temperature distribution. (2) We coated the print bed with glue (UHU® stic, Germany) made almost entirely of natural ingredients (i.e., 98% starch and water), to improve attachment without the risk of contaminating the test structures for biochemical applications. (3) Finally, we added sacrificial material to the edges of the print object to provide extra contact area to the build plate to reduce warping. The extended bottom surface was meant to hold down the edges of the part during printing and absorbs most of the initial warping. This brim can be incorporated during the design process using 3D printing software, such as Cura, Eiger, or Simplify 3D®. Note that this type of structure is easily removed after printing. In this study, the brim was added using the "brim" tool under "Platform adhesion types" (instead of "Raft" or "Skirt" options), using CURA 15.04 (Ultimaker, the Netherlands)

B. Fundamentals and bonding procedure

Organic solvent bonding is commonly used to seal up microfluidic devices. This involves the use of specific organic solvents to break down polymer chains at the surface, which then diffuse across the dissolved layer resulting in the extensive intertwining of chains between surfaces to create a permanent bond. This mechanism makes it possible to realize a strong bond even at low temperatures using a minimum of equipment. It also eliminates the clogging and channel deformation associated with adhesive bonding or thermal fusion bonding.

Organic solvent bonding was used in this study to bond PMMA and ABS. We selected ethanol as a solvent because it is nontoxic and dissolves PMMA substrates (Sinrich, Taichung, Taiwan) without affecting their optical properties.[35] In previous studies, we adopted spin coating to distribute the solvent over the surfaces to be bonded. We had considerable success bonding various thermoplastic combinations, including PMMA/PMMA, PMMA/PC, PMMA/PET, and even PMMA/PLA.[36,37] Specifically, we employed a sandwich spin coating strategy, in which a solvent layer is deposited between two substrates, whereupon centrifugal forces, surface tension, and capillary forces are used to produce a uniform, bubble-free layer of solvent,

resulting in a strong bond between thermoplastic materials. However, this process caused the wasting of more than 90% of the material.[38] Thus, in this study, we adopted a spray coating technique for the distribution of solvent. This simple method involves the spraying of ethanol solution (95%, BDH 1158-4LP, VWR International) via a very fine sprayer nozzle (500 μm) (YS 301-220, Taiwan) to produce a fine aerosol for the simultaneous coating of the PMMA and ABS surfaces. This technique has considerable potential, particularly for large-scale production, due to the fact that it is not limited by the size of the substrate and uses very little solvent. Once the PMMA and ABS surfaces are coated with ethanol solution, they are brought into contact and fixed using binder clips before being placed within a UV machine (UV XLite500Q, OPAS, Taichung, Taiwan) to undergo irradiation (84 s). Under the heat resulting from UV exposure (365 nm; intensity = 80 mW/cm^2; temperature maintained in the range from 55 °C to 60 °C), the ethanol solution dissolves the PMMA substrate to create acrylate monomers. This phenomena was described and explained by Hoogenboom *et al.*[35] Due to similarities in the solubility parameter (δ) of the two materials [δ(ABS) ∼ 20.4;[39] δ (PMMA) ∼ 20.1],[20] the resulting acrylate monomers diffuse across the boundary between the thermoplastics and undergo crosslinking. This leads to the instantaneous formation of a permanent bond between the PMMA and ABS substrates. However, residual stress resulting from an increase in temperature from 55 °C to 60.5 °C during UV exposure for 84 s, measured by a thermometer (TES 1384, TES Electrical Electronic Corp., Taiwan), increases the likelihood of bond failure. We therefore used an oven (DK-600DT, L.M.I. Co., Ltd, Taiwan) to initiate post-annealing immediately after UV exposure, with the aim of relieving residual stress and thereby improving bonding strength. We used an annealing temperature of 55 °C, which is below the glass transition point of PMMA (Tg = 105–122 °C)[20] and ABS (Tg ∼ 105 °C),[26,27] thereby preventing channel deformation. The overall bonding procedure is illustrated in Fig. 1. In the supplementary material, we fabricated a microfluidic chip with S-microchannel to investigate the influence of different bonding parameters, such as UV exposure time, spray coating, and post-annealing step on bonding quality. Leakage tests, burst tests, and SEM tests were used to characterize the bonded microfluidic chips. As a result, at least eight bars for the bonding strength of ABS/PMMA was achieved.

C. Practical applications of microfluidic chips

In this section, we describe the fabrication of two types of hybrid microfluidic chip (a 3D SAR-based passive micromixer and an integrated microfluidic chip), using the method described above. ABS objects were printed using the parameters in Table I in conjunction with the methods mentioned earlier for the prevention of warping and/or detachment. PMMA substrates (75 × 56 × 2 mm^3) were used to cover the open structures on the printed ABS substrates. Prior to bonding, the PMMA and ABS substrates were ultrasonically cleaned (LEO-2003S, Leo Ultrasonic Co. Ltd, Taipei,

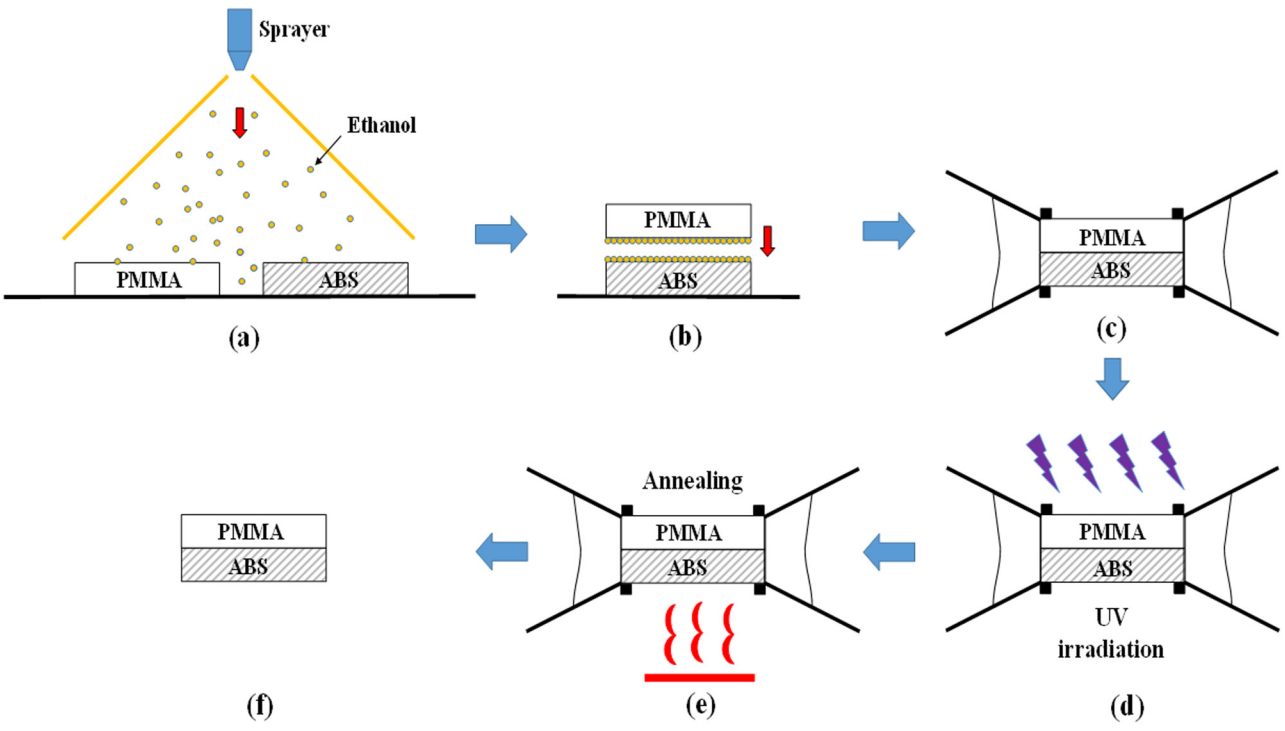

FIG. 1. Overall bonding procedure: (a) Sprayer used to apply ethanol solution to PMMA and printed ABS substrates; (b) two substrates were then brought into contact with each other; (c) binder clips were used to fix the assembly; (d) UV irradiation; (e) post annealing for relief of residual stress; and (f) bonded microfluidic chip.

TABLE I. Print parameters of ABS objects used in this study.

Parameter	Value
Layer thickness	0.2 mm
Wall thickness	1.2 mm
Top/bottom layer thickness	1 mm
Infill density	30%
Platform adhesion	Brim

Taiwan) using distilled water for 10 min. Syringe pumps (NE-1000 and NE-4000 model, New Era Pump Systems Inc., USA) were employed to introduce liquids into the microfluidic chips. After the experiments, the bonded chips were affixed to the stage of a stereomicroscope (SL-730, SAGE Vision, Taiwan) to enable optical analysis using a digital camera (650D, Global Canon).

1. Fabrication of 3D SAR-based passive micromixer

Uniform mixing in microfluidic devices is hindered by laminar flow in the microchannels. A number of novel methods (active and passive) have been developed to enhance mixing efficiency. Active micromixers provide excellent mixing performance (MP) and control over flow by employing external energy sources to create perturbations in the reagent. However, these schemes are not easily integrated within microfluidic systems and the manufacturing costs tend to be high. Passive micromixers depend entirely on the geometric design of the channel structure to impose chaotic advection. This type of mixing is incorporated within the system during fabrication. The fact that the mixing process is not externally controlled by the user greatly simplifies fabrication, integration, and operations. SAR is the passive micromixer with the highest mixing efficiency, thanks to the splitting and recombining of two streams to optimize diffusion.[40] This type of micromixer is often fabricated via computer numerical control (CNC) milling in conjunction with an engraving process.[41,42] In this study, 3D printing was used to create an SAR-based passive micromixer with microchannels designed to produce 90° flow rotation, resulting in a folding of the stream followed by splitting and recombining to enhance mixing efficiency and enable the use of multiple tubing connectors simultaneously. Compared to existing methods, the proposed scheme greatly simplifies the fabrication process by creating complicated 3D structure and connection ports in a single 3D printing step to reduce manufacturing time and costs.

We also sought to illustrate that the use of transparent material is insufficient for optical observations in 3D-printed microfluidic chips. This was achieved by fabricating the proposed micromixer using two approaches for comparison. (1) We used transparent ABS to print the entire microfluidic chip and (2) we created a hybrid chip in which open structures were printed on white ABS material, and then sealed with a PMMA substrate using the proposed bonding method. The microchannels in both devices were identical in terms of dimensions (i.e., the width is 900 μm with various depths). Each chip was configured with four embedded tubing connectors to resolve the world-to-chip (or macro-to-micro) interface problem commonly encountered when using microfluidic devices. Figure 2(a) illustrates the design of the hybrid 3D microfluidic mixer with embedded connectors.

Regarding to color mixing, we employed an end-point detection experiment, which was described in detail from previous article[43] to evaluate the mixing performance (MP) based on the following equation:

$$\mathrm{MP} = 1 - \frac{1}{\bar{m}}\sqrt{\frac{\sum_{i=1}^{n}(m_i - \bar{m})^2}{n}},$$

where n is the number of points, m_i is the concentration at the point, and $\bar{m}$ is the average concentration.[44] In the mixing experiment on 3D SAR-based passive micromixer, three food dyes of different colors (red, yellow, and blue) were injected into the micromixer at different flow rates: red (0.5 ml/min), yellow (1.0 ml/min), and blue (0.5 ml/min). The hybrid microfluidic device was affixed to the stage of a stereomicroscope (SL-730, SAGE Vision, Taiwan) and a digital camera (650D, Global Canon) was used to capture images of the mixing process for further analysis. The resolution of the figure is 1920×1280, so each pixel represents 8.3 μm in the x-direction and 8.4 μm in the y-direction. The mixing process took place in two steps: step (1) is the mix of red (blue) and yellow dyes to create orange (green) stream and step (2) is the mix of orange and green dyes to create dark brown stream. Figure 2(b) illustrates the mixing routes for each step [the red route for step (1) and the black route for step (2)]. The black dots are the places at which two different dyes start to mix with each other. The white dots represent for the places which pictures will be took for MP analysis. The total length of microchannels in step (1) is 32.8 mm, and for step (2) is 34 mm. Evaluation of MP was achieved by examining on each step under steady state mixing conditions.

2. Fabrication of integrated microfluidic chip

3D printing enables the fabrication of highly complex structures without limitations pertaining to range, aspect ratio, or spatial integration. The proposed bonding method makes it possible to fully exploit these complex designs in the creation of microfluidic chips. In the following, we describe an integrated microchip comprising a 3D SAR-based micro mixer and double-emulsion generator with five tubing connectors. Figure 3(a) illustrates the layout of the hybrid chip with embedded tubing connectors for inlets/outlets. Microchannels were printed on an ABS substrate ($75 \times 56 \times 7.5$ mm^3) and then sealed using PMMA via the proposed bonding method. We adopted water-in-oil-in-water (W/O/W) as the configuration of final emulsion products. The inner water phase was a mixture of yellow and blue food dyes passing through the SAR-mixer zone at a flow rate of 0.2 (ml/min). Oleic acid was used as the oil phase (outer phase), which was injected into the first T-junction at a flow rate of 1.0 (ml/min) to create single droplets. The continuous phase was distilled water, which was pumped into the second T-junction at a flow rate of 0.6 (ml/min), where it was broken up by immiscible single water-in-oil (W/O) droplets to create double-emulsion droplets. Double-emulsion droplets (W/O/W) were intended to be the final products of this hybrid chip; however, we intentionally created a number of single droplets (W/O) using the same device to illustrate the difference between them. By halting the flow of continuous phase (distilled water) into the second T-junction, it was possible to form single

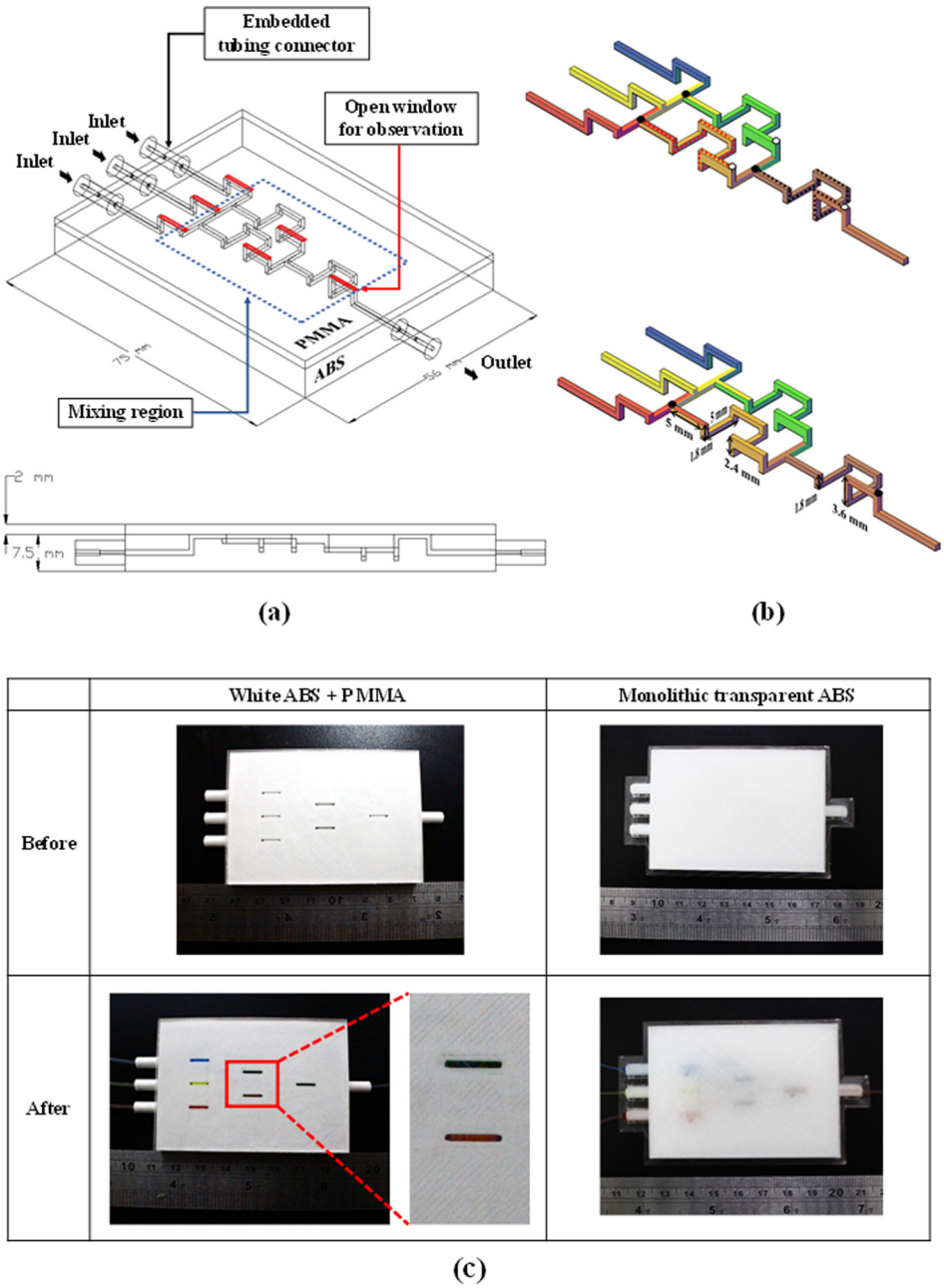

FIG. 2. (a) Design layout of hybrid 3D SAR-based passive micromixer with embedded connectors; (b) 3D SAR-based passive micromixer; (c) images illustrating the mixing performance of the two 3D SAR-based passive micromixers (identical dimensions): hybrid chip comprising white ABS and PMMA, and a "transparent" monolithic ABS chip.

droplets and store them in a Petri dish, before reactivating the stream of continuous phase to generate double-emulsion droplets.

III. RESULTS AND DISCUSSION

A. Transparency and mixing performance of 3D SAR-based passive micromixer

Figure 2(c) illustrates the mixing performance of the two 3D SAR-based passive micromixers (with identical dimensions), including (1) a hybrid chip comprising white ABS and PMMA and (2) a "transparent" monolithic ABS chip. The images were obtained after the three streams were injected into the micromixer at different flow rates: red (0.5 ml/min), yellow (1.0 ml/min), and blue (0.5 ml/min) to form streams of orange and green, and finally dark brown liquid. From the experiment results, the proposed micromixer is able to achieve MP of approximately 90% [92% for step (1) and 89% for step (2)] within 5 s and in the mixing region which was marked as the blue dashed line in Fig. 2(a). The hybrid chip of

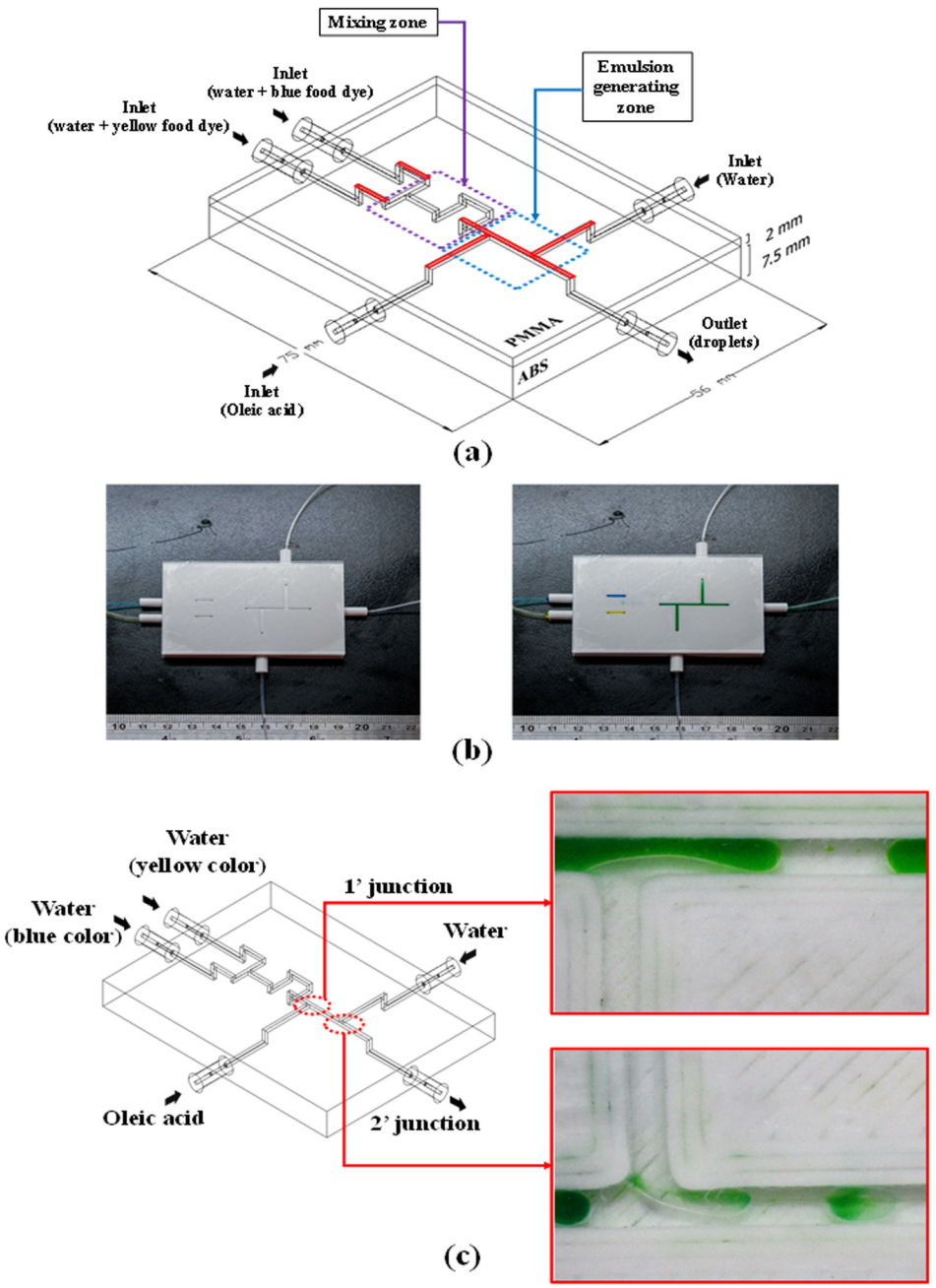

FIG. 3. (a) Design layout of integrated microfluidic chip; (b) experiment results of leakage test and mixing performance in various locations along the ABS/PMMA integrated microfluidic chip; and (c) double-emulsion generated using the proposed device.

ABS/PMMA clearly showed the colors of the various flows; however, the "transparent" chip did not allow such observations due to the fact that it was actually translucent after printing. The transparent tubing was easily connected to the ABS connectors. Experiment results led to the following observations: (1) we succeeded in fabricating a low-cost 3D SAR-based passive micromixer with high mixing performance; (2) the inclusion of multiple printed tubing connectors greatly facilitated tubing assembly without concerns about leakage, tubing assembly integrity, or reliability; and (3) mixing performance could be quantified from the PMMA side using a reflective optical system. A transmittance spectra of fabricated windows is shown in Fig. S6 in the supplementary material; the optical transmission of fabricated windows was >90% in the visible range; and it was 89% at 352 nm, 84% at 325 nm, and 76% at 298 nm.

B. Performance of integrated microfluidic chip in mixing and double-emulsion generation

Before generating double-emulsion droplets, yellow and blue food dyes were introduced into the device to test for the occurrence of leakage. As shown in Fig. 3(b), no leakage was observed during mixing.

Figure 3(c) illustrates the generation of a double-emulsion (W/O/W) following the injection of yellow and blue food dyes, oleic acid, and distilled water into the microfluidic chip at specific flow rates. The overall process can be divided into three phases, corresponding to three areas of the hybrid chip: Phase 1 (zone 1) is the mixing of yellow and blue food dyes to form a stream of green liquid; Phase 2 (zone 2) is the creation of single-emulsion droplets; and Phase 3 (zone 3) is the generation of double-emulsion droplets. The droplets were formed at a rate of 2 droplet/s in zone 1 and 1 droplet/s in zone 2. An image of two types of droplet (single- and double-emulsion) generated using the proposed hybrid chip and held in a Petri dish is shown in Fig. S7 in the supplementary material.

Our experiment results clearly show that a hybrid microfluidic chip can be created cheaply and easily using the proposed bonding method. To understand the bonding quality, SEM and microscope were used to investigate the cross-sectional area as well as to measure the dimension of the printed chips. Figure 4(a) shows the cross-sectional area of the ABS/PMMA bonded chip with S-microchannel, and the substrate above the dashed line is PMMA and the substrate below the dashed line is ABS. Figures 4(b) and 4(c) show the measured dimension of the channel on the ABS substrate. This scheme takes full advantage of 3D printing to create multiple components with different functions and degrees of complexity within a single chip. The excellent optical clarity on the PMMA side and multiple

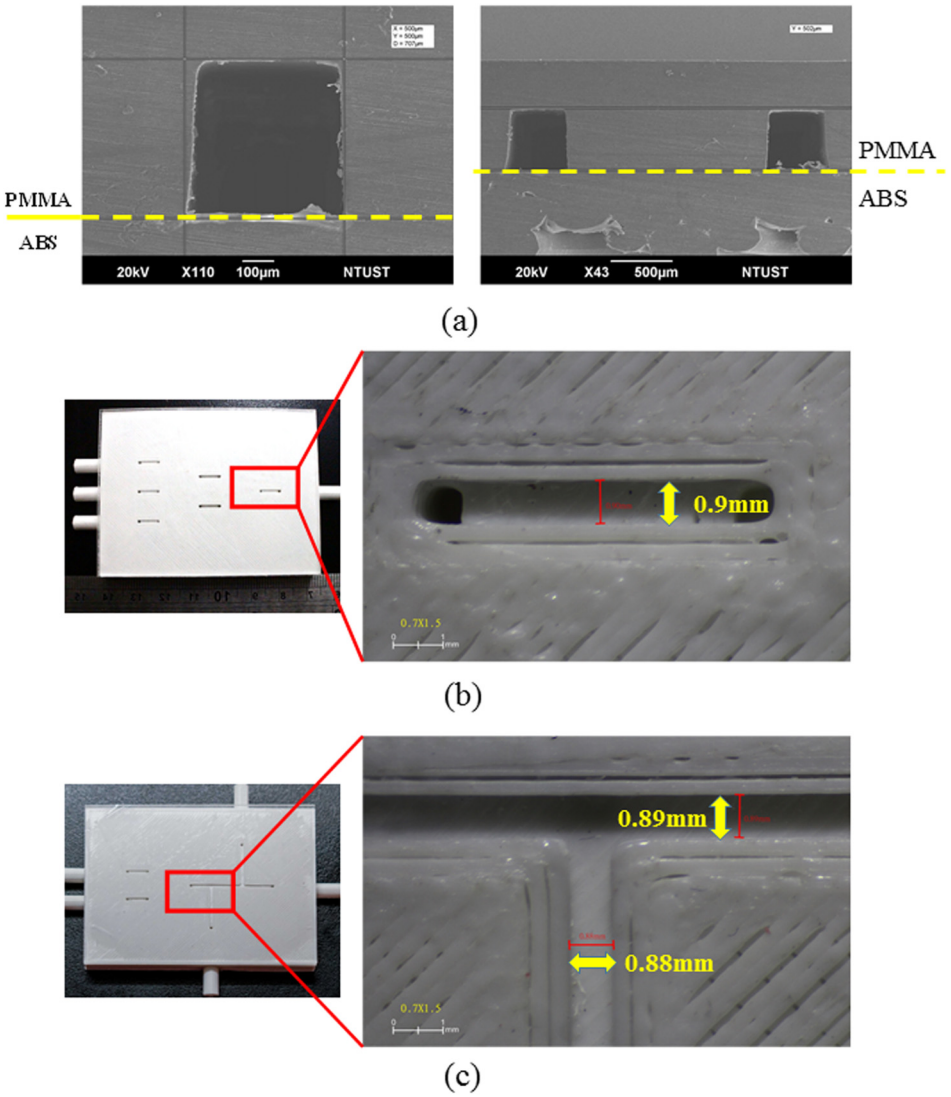

FIG. 4. (a) The SEM shows the cross-sectional investigation of the bonded chip with S-microchannel; (b) the measured dimension of the channel of 3D SAR-based passive micromixer; and (c) the measured dimension of the double-emulsion generator.

embedded tubing connectors make it far easier to produce double-emulsions (W/O/W), which are very useful in a number of biological and industrial applications, such as drug delivery, cosmetics, and food products. The proposed scheme also facilitates the assembly of tubing connectors. The ability to forego the use of UV glues, fittings, and polydimethylsiloxane (PDMS) elements with punched holes all but eliminates interface problems, including cost, reliability, clogging, and contamination.

IV. CONCLUSIONS

3D printing has attracted considerable interest in the fabrication of microfluidic devices, thanks to its low cost, rapid prototyping, and ability to realize complex structures.[14] However, most existing devices lack the optical transparency required for tasks involving quantification. In this study, we developed a novel fabrication process for the creation of hybrid microfluidic devices using substrates of ABS and PMMA. Several methods were adopted to prevent warping during FDM printing process. Annealing was also used to reduce residual stress and thereby improve bonding performance. In this study, we fabricated two microfluidic chips to evaluate the efficacy of the proposed approach: 3D SAR-based passive micromixer, an integrated microchip comprising a mixer system, and double-emulsion generator. Experiment results revealed the following: (1) the proposed scheme can be used to integrate multiple components with diverse functions and various degrees of complexity within a single microchip. The proposed fabrication scheme is far simpler, faster, and less expensive than convention methods; (2) the 3D printing of multiple tubing connectors (i.e., user interface) greatly facilitates setting up the device for experiments but eliminates concerns pertaining to leakage, contamination, tubing assembly integrity, and reliability; (3) the transparency of the proposed device far exceeds that of other 3D-printed devices, thereby making it possible to characterize the mixing performance and/or generation of droplets using a reflection-based optical system from the PMMA side. As mentioned in a previous paper,[36] the creation of sub-micro/nanochannels on the PMMA side using other techniques (e.g., micromilling, laser machining) could help to overcome limitations pertaining to the current resolution of 3D printers for applications requiring channels of particularly high precision.

SUPPLEMENTARY MATERIAL

See the supplementary material for the characterization of bonding protocol (including Tables S1 and S2, Figs. S1, S2, S3, S4, and S5), the transmittance spectra of fabricated windows (Fig. S6), and the image of single- and double-emulsion droplets generated from the proposed hybrid microfluidic chip (Fig. S7).

ACKNOWLEDGMENTS

This work was funded by the Ministry of Science and Technology (MOST No. 107-2221-E-011-059) and the Mechanical Engineering Department of National Taiwan University of Science and Technology (NTUST).

REFERENCES

[1]3D printing market by offering (printer, material, software, service), process (binder jetting, direct energy deposition, material extrusion, material jetting, powder bed fusion), application, vertical, and geography—global forecast to 2023.
[2]K. B. Anderson, S. Y. Lockwood, R. Scott Martin, and D. M. Spence, "A 3D printed fluidic device that enables integrated features," Anal. Chem. **85**, 5622–5626 (2013).
[3]A. I. Shallan, P. Smejkal, M. Corban, R. M. Guijt, and M. C. Breadmore, "Cost-effective three-dimensional printing of visibly transparent microchips within minutes," Anal. Chem. **86**, 3124–3130 (2014).
[4]W. Lee, D. Kwon, B. Chung, G. Y. Jung, A. Au, A. Folch, and S. Jeon, "Ultrarapid detection of pathogenic bacteria using a 3D immunomagnetic flow assay," Anal. Chem. **86**, 6683–6688 (2014).
[5]W. Lee, D. Kwon, W. Choi, G. Y. Jung, A. K. Au, A. Folch, and S. Jeon, "3D-printed microfluidic device for the detection of pathogenic bacteria using size-based separation in helical channel with trapezoid cross-section," Sci. Rep. **5**, 7717 (2015).
[6]G. Comina, A. Suska, and D. Filippini, "PDMS lab-on-a-chip fabrication using 3D printed templates," Lab Chip **14**, 424–430 (2014).
[7]H. N. Chan, Y. Chen, Y. Shu, Y. Chen, Q. Tian, and H. Wu, "Direct, one-step molding of 3D-printed structures for convenient fabrication of truly 3D PDMS microfluidic chips," Microfluid. Nanofluid. **19**, 9–18 (2015).
[8]Y. Hwang, O. H. Paydar, and R. N. Candler, "3D printed molds for non- planar PDMS microfluidic channels," Sens. Actuators, A **226**, 137–142 (2015).
[9]K. Kang, S. Oh, H. Yi, S. Han, and Y. Hwang, "Fabrication of truly 3D microfluidic channel using 3D-printed soluble mold," Biomicrofluidics **12**, 014105 (2018).
[10]P. J. Kitson, M. H. Rosnes, V. Sans, V. Dragone, and L. Cronin, "Configurable 3D-Printed millifluidic and microfluidic "lab on a chip" reactionware devices," Lab Chip **12**, 3267–3271 (2012).
[11]P. J. Kitson, S. Glatzel, W. Chen, C.-G. Lin, Y.-F. Song, and L. Cronin, "3D printing of versatile reactionware for chemical synthesis," Nat. Protoc. **11**, 920–936 (2016).
[12]F. Li, P. Smejkal, N. P. Macdonald, R. M. Guijt, and M. C. Breadmore, "One-step fabrication of a microfluidic device with an integrated membrane and embedded reagents by multimaterial 3D printing," Anal. Chem. **89**, 4701–4707 (2017).
[13]G. Gaal, M. Mendes, T. P. de Almeida, M. H. O. Piazzetta, Â. L. Gobbi, A. R. Jr., and V. Rodrigues, "Simplified fabrication of integrated microfluidic devices using fused deposition modeling 3D printing," Sens. Actuators, B **242**, 35–40 (2017).
[14]N. Bhattacharjee, A. Urrios, S. Kang, and A. Folch, "The upcoming 3D-printing revolution in microfluidics," Lab Chip **16**, 1720–1742 (2016).
[15]C. Chen, B. T. Mehl, A. S. Munshi, A. D. Townsend, D. M. Spence, and R. Scott Martin, "3D-printed microfluidic devices: Fabrication, advantages and limitations—a mini review," Anal. Methods Adv. Methods Appl. **8**, 6005–6012 (2016).
[16]S. Takenaga, B. Schneider, E. Erbay, M. Biselli, T. Schnitzler, M. J. Schöning, and T. Wagner, "Fabrication of biocompatible lab-on-chip devices for biomedical applications by means of a 3D-printing process," Phys. Status Solidi A **212**, 1347–1352 (2015).
[17]J. D. Wardyn, C. Sanderson, L. E. Swan, and M. Stagi, "Low cost production of 3D-printed devices and electrostimulation chambers for the culture of primary neurons," J. Neurosci. Methods **251**, 17–23 (2015).
[18]G. I. Salentijn, P. E. Oomen, M. Grajewski, and E. Verpoorte, "Fused deposition modeling 3d printing for (bio)analytical device fabrication: Procedures, materials, and applications," Anal. Chem. **89**, 7053–7061 (2017).
[19]V. Bertana, C. Potrich, G. Scordo, L. Scaltrito, S. Ferrero, A. Lamberti, F. Perrucci, C. F. Pirri, C. Pederzolli, M. Cocuzza, and S. L. Marasso, "3D-printed microfluidics on thin poly(methyl methacrylate) substrates for genetic applications," J. Vac. Sci. Technol. B **36** (2018).
[20]C.-W. Tsao and D. L. DeVoe, "Bonding of thermoplastic polymer microfluidics," Microfluid. Nanofluid. **6**, 1–16 (2009).

[21]D. J. Guckenberger, T. E. de Groot, A. M. D. Wan, D. J. Beebe, and E. W. K. Young, "Micromilling: A method for ultra-rapid prototyping of plastic microfluidic devices," Lab Chip **15**, 2364–2378 (2015).
[22]P.-C. Chen, Y.-P. Chang, R.-H. Zhang, C.-C. Wu, and G.-R. Tang, "Microfabricated microfluidic platforms for creating microlens array," Opt. Express **25**, 16101–16115 (2017).
[23]C. Matellan, and A. E. del Río Hernández, "Cost-effective rapid prototyping and assembly of poly(methyl methacrylate) microfluidic devices," Sci. Rep. **8**, 6971 (2018).
[24]K. Yamasaki, S. Juodkazis, S. Matsuo, and H. Misawa, "Three-dimensional microchannels in polymers: One-step fabrication," Appl. Phys. A **77**, 371–373 (2003).
[25]J. Wu, R. Chantiwas, A. Amirsadeghi, S. A. Soper, and S. Park, "Complete plastic nanofluidic devices for DNA analysis via direct imprinting with polymer stamps," Lab Chip **11**, 2984–2989 (2011).
[26]M. Rahman, N. R. Schott, and L. K. Sadhu, "Glass transition of ABS in 3D printing," in COMSOL Conference, Boston, MA, 2016.
[27]G. S. Ananthapadmanabha and V. V. Deshpande, "Thermal properties of acrylonitrile butadiene styrene composites," Indian J. Adv. Chem. Sci. **S1**, 279–282 (2016).
[28]S. Olivera, H. B. Muralidhara, K. Venkatesh, K. Gopalakrishna, and C. S. Vivek, "Plating on acrylonitrile–butadiene–styrene (ABS) plastic: a review," J. Mater. Sci. **51**, 3657–3674 (2016).
[29]F. S. Kamelian, E. Saljoughi, P. S. Nasirabadi, and S. M. Mousav, "Modifications and research potentials of acrylonitrile/butadiene/styrene (ABS) membranes: A review," Polym. Compos. **39**, 2835–2846 (2018).
[30]E. Bartolomé, B. Bozzo, P. Sevilla, O. Martínez-Pasarell, T. Puig, and X. Granados, "ABS 3D printed solutions for cryogenic applications," Cryogenics **82**, 30–37 (2017).
[31]J. Hyde, M. MacNicol, A. Odle, and E. Garcia-Rill, "The use of three-dimensional printing to produce in vitro slice chambers," J. Neurosci. Methods **238**, 82–87 (2014).
[32]Y. Ramot, M. Haim-Zada, A. J. Domb, and A. Nyska, "Biocompatibility and safety of PLA and its copolymers," Adv. Drug Delivery Rev. **107**, 153–162 (2016).
[33]R. P. Rimington, A. J. Capel, S. D. R. Christie, and M. P. Lewis, "Biocompatible 3D printed polymers via fused deposition modelling direct C2C12 cellular phenotype in vitro," Lab Chip **17**, 2982–2993 (2017).
[34]D. H. Rosenzweig, E. Carelli, T. Steffen, P. Jarzem, and L. Haglund, "3D-printed ABS and PLA scaffolds for cartilage and nucleus pulposus tissue regeneration," Int. J. Mol. Sci. **16**, 15118–15135 (2015).
[35]R. Hoogenboom, C. Remzi Becer, C. Guerrero-Sanchez, S. Hoeppener, and U. S. Schubert, "Solubility and thermoresponsiveness of PMMA in alcohol-water solvent mixtures," Aust. J. Chem. **63**, 1173–1178 (2010).
[36]L. H. Duong and P.-C. Chen, "Novel solvent bonding method for creation of a three-dimensional, non-planar, hybrid PLA/PMMA microfluidic chip," Sens. Actuators A **280**, 350–358 (2018).
[37]P.-C. Chen and L. H. Duong, "Novel solvent bonding method for thermoplastic microfluidic chips," Sens. Actuators, B **237**, 556–562 (2016).
[38]N. Sahu, B. Parija, and S. Panigrahi, "Fundamental understanding and modeling of spin coating process: A review," Indian J. Phys. **83**, 493–502 (2009).
[39]A. F. M. Barton, "Solubility parameters," Chem. Rev. **75**, 731–753 (1975).
[40]G. Cai, L. Xue, H. Zhang, and J. Lin, "A Review on Micromixers," Micromachines **8**, 274 (2017).
[41]V. Viktorov and M. Nimafar, "A novel generation of 3D SAR-based passive micromixer: efficient mixing and low pressure drop at a low Reynolds number," J. Micromech. Microeng. **23**, 055023 (2013).
[42]V. Viktorov, M. R. Mahmud, and C. Visconte, "Numerical study of fluid mixing at different inlet flow-rate ratios in Tear-drop and Chain micromixers compared to a new H-C passive micromixer," Eng. Appl. Comp. Fluid Mech. **10**, 182–192 (2016).
[43]P.-C. Chen, C.-W. Pan, and Y.-L. Kuo, "Performance characterization of passive micromixer with dual opposing strips on microchannel walls," Chem. Eng. Process. **93**, 27–33 (2015).
[44]Y. Fang, Y. Ye, R. Shen, P. Zhu, R. Guo, Y. Hu, and L. Wu, "Mixing enhancement by simple periodic geometric features in microchannels," Chem. Eng. J. **187**, 306–310 (2012).